Fuel and Moderator Temperature Feedback of MOX Fuel for DARWIN Reactor Core

Anže Mihelčič [1, 2,*], Dušan Čalič[1], Tanja Goričanec[1, 2], Luka Snoj[1, 2]

[1]Jožef Stefan Institute, Jamova cesta 39, Ljubljana, Slovenia;
[2]Faculty of Mathematics and Physics UL, Jadranska cesta 19, Ljubljana, Slovenia

DOI: 10.5281/zenodo.20803950

ABSTRACT

This work evaluates fuel and moderator temperature reactivity feedback for mixed oxide (MOX) fuel in the Dispatchable Adaptive Reactor With Interchangeable compoNents (DARWIN), a modular reactor concept requiring inherently safe operation through negative temperature coefficients. Temperature-dependent reactivity coefficients are calculated for various uranium enrichments, UO_2 weight fractions in UO_2–PuO_2 mixtures, and boron concentration in the coolant.

Monte Carlo were performed with Serpent 2.2.0 using ENDF/B-VII.1 nuclear data, based on a two-dimensional core model with 37 hexagonal MOX assemblies each consisting of 127 identical fuel pins. Moderator temperature coefficients (α_m) were computed for moderator temperatures between 560 K and 600 K, while fuel temperature coefficients (α_f) were evaluated from 560 K to 1080 K. Both α_m and α_f remain negative across all examined configurations, confirming stable feedback behaviour. The magnitude of α_m increases for lower uranium enrichments and higher UO_2 weight fractions, driven by temperature-induced variations in radiative capture reaction rates. Increased boron concentration reduces magnitude of α_m without resulting in positive values. The fuel temperature coefficient becomes less negative with increasing enrichment and decreasing UO_2 weight fraction, consistent with decrease in radiative capture reaction rate with temperature increase.

The study provides parametric feedback trends and reference coefficient data to support future MOX-fuelled DARWIN core design and safety assessment.

Keywords: DARWIN, flexible reactor, temperature effects, MOX fuel

1. INTRODUCTION

The concept of the Dispatchable Adaptive Reactor With Interchangeable compoNents (DARWIN) [1] provides a solution to the urgent and emergency needs of the present and future world. Its modular design enables responses to specific needs and applications such as flood water pumping, district heating, desalination, radioisotope production, and load-following electricity generation, which was already indetified as possible use od Small Modular Reactors (SMRs) [2]. The reactor will consist of different core modules (e.g., fuel elements, reactivity control, neutron reflector, isotope production) and secondary side modules (e.g., flood water pumping, heat production), which should be optimised for particular uses. The main reactor parameters, such as nominal power, operating temperature, and pressure, are not defined yet because they depend on the reactor type and its intended application.

The selection of nuclear fuel is based on the physical and safety limitations of specific applications, such as the requirement for negative temperature reactivity feedback and differing needs for radioisotope production, heat generation, or operation in load-following mode. This paper focuses on MOX fuel, identified as a promising candidate in [3], and presents a more detailed physics analysis of its temperature feedback behaviour, including reaction rates and spectral effects for different UO_2 weight

*anze.mihelcic@ijs.si

fractions and uranium enrichments. This analysis allows the identification of key operational limits and characteristic trends of the temperature feedback.

Temperature effects were evaluated using temperature feedback coefficients, defined as

$$\alpha_j = \frac{\partial \rho}{\partial T_j}, \tag{1}$$

where α_j is the temperature feedback coefficient for material j (fuel or moderator), ρ is the reactivity, and T_j is the temperature of material j. In general, these coefficients are not constant and may depend on temperature. To estimate temperature dependence, the difference between two discrete temperatures is used:

$$\alpha_j(T_{i,j}) = \frac{\rho(T_{i+1/2,j}) - \rho(T_{i-1/2,j})}{T_{i+1/2,j} - T_{i-1/2,j}}, \tag{2}$$

where $T_{i,j}$ is the temperature between two neighbouring temperatures $T_{i\pm1/2,j}$, which were used in the calculations.

Reaction rates were calculated at different moderator and fuel temperatures for two reactions: a) total fission (MT number 18) and b) radiative capture (MT number 102). The reaction rate values in the fuel of the central fuel assembly are presented.

Section 2 presents the computational model, including geometry and material description. Sections 3 and 4 present the results of the moderator and fuel temperatures feedback coefficients, and Section 5 summarises the main findings.

2. COMPUTATIONAL MODEL

For this analysis, a two-dimensional core was assumed, containing only fuel pins assembled in hexagonal fuel assemblies and surrounded by a band of water only, which acts as a reflector, as shown in Figure 1. The hexagonal arrangement of fuel pins and assemblies enables a more uniform power distribution across the core compared with fuel pins in a square lattice. Calculations were performed using the Serpent 2.2.0 Monte Carlo code [4] with the ENDF/B-VII.1 nuclear data library [5], 300 inactive, 1000 active cycles, and 10^5 neutrons per cycle. Calculations resulted in a relative statistical uncertainty of approximately 5 pcm in k_{eff} and approximately 3×10^{-1} % for the neutron flux per energy group.

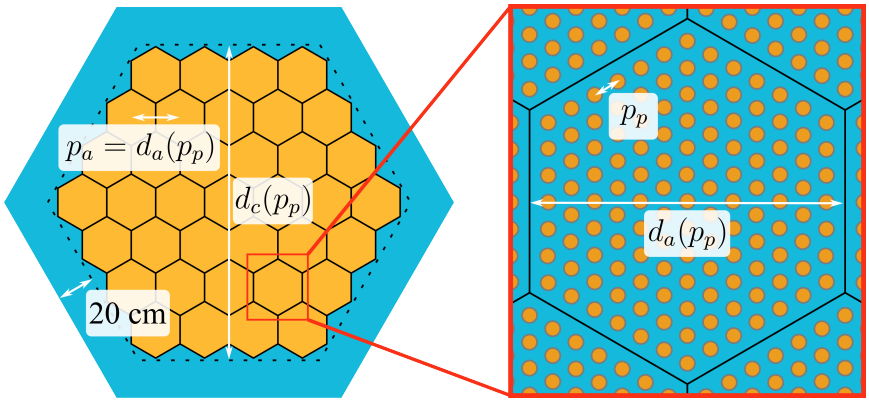

Figure 1. Schematic representation of the reactor core geometry used in the simulations. The core (right) consists of 37 hexagonal fuel assemblies, separated by an assembly pitch p_a, and is surrounded by a 20 cm thick water reflector. Each fuel assembly (left) contains 127 fuel rods arranged in a hexagonal lattice with a pin pitch p_p. The assembly size d_a, the core size d_c, and the assembly pitch p_a are derived from the pin pitch p_p.

The core consists of 37 fuel assemblies, each with 127 identical fuel pins. Each fuel pin contains a central MOX fuel pellet, a helium-filled gap, and Zircaloy-4 cladding, surrounded by water acting as both coolant and moderator. In this study, the distance between fuel pins (pin pitch) was set to $p_p = 1.4\,\text{cm}$, resulting in an assembly size of $d_a = 16.2\,\text{cm}$ and a core size of $d_c = 102.7\,\text{cm}$. The value $p_p = 1.4\,\text{cm}$ was selected because, at this pitch, the core is approximately ideally moderated at room temperature and becomes under-moderated at higher temperatures [6, 7].

Simulations were conducted at various fuel and moderator temperatures and with different boron concentrations in the coolant. The temperature, pressure, and boron concentration values are typical for pressurised water reactors (PWRs). Water density data were taken from [8]. The isotope composition of the PuO_2 component used in the simulations was taken from [9]. The corresponding plutonium vector was: ^{238}Pu, 0.05 %; ^{239}Pu, 93.50 %; ^{240}Pu, 6.00 %; ^{241}Pu, 0.40 %; and ^{242}Pu, 0.05 %. For the UO_2 component, the isotopes ^{234}U, ^{235}U, ^{236}U, and ^{16}O are assumed, with isotopic composition depending on the uranium enrichment.

3. MODERATOR TEMPERATURE FEEDBACK

Change in the moderator temperature was implemented by adjusting:

- the moderator material temperature,
- the moderator density, and
- the thermal scattering data for hydrogen in water.

As the fuel temperature does not affect the moderator temperature feedback, and the reactivity coefficient remains unchanged regardless of the fuel temperature, the fuel temperature was fixed at 300 K. The moderator temperature was varied from 560 K to 600 K in increments of 10 K.

Figure 2 shows the temperature dependence of the moderator temperature reactivity feedback coefficient α_m for various cases:

- 3 % and 20 % enriched uranium,
- UO_2 weight fractions of 96 % (data from [9]) and 78 %, generated from the 96 % case using an arbitrarily chosen 6 % step (only the first and last values are shown),
- boron concentrations of 0 ppm, 1000 ppm, and 2500 ppm.

In general, α_m becomes more negative (i.e. the feedback becomes stronger, the impact on reactivity is larger) as the moderator temperature increases. This behaviour can be explained by different temperature trends in the fission and radiative capture reaction rates, as illustrated in Figure 3, which shows the sum of reaction rates for the nuclides ^{235}U, ^{238}U, ^{239}Pu, ^{240}Pu, ^{241}Pu, and ^{242}Pu. The highest rate of fission reactions (an order of magnitude larger than for other nuclides) occurs on ^{235}U, ^{239}Pu, and ^{241}Pu, while the highest rate of capture reactions occurs on ^{240}Pu and ^{242}Pu.

It can be seen that the value of α_m is more negative (the effect is stronger) for lower uranium enrichment and a higher UO_2 weight fraction, which can be explained by temperature-induced changes in reaction rates, as shown in Figure 3. The main contribution to fission originates from ^{235}U, ^{239}Pu, and ^{241}Pu, which dominate power production due to their large fission cross sections. In contrast, the strongest radiative capture occurs in ^{240}Pu and ^{242}Pu, which effectively act as absorbers. As moderator temperature increases, the spectrum becomes slightly harder, reducing the thermal flux and modifying resonance self-shielding in both uranium and plutonium isotopes. This leads to a relatively stronger increase in capture rates in ^{240}Pu and ^{242}Pu compared to the change in fission rates of ^{235}U, ^{239}Pu, and ^{241}Pu, particularly at lower uranium enrichment and higher UO_2 weight fraction. The linear fits in Figure 3 show that, for the 3 % enrichment case, the capture-rate slope is even positive compared to the capture-rate slope for the 20 % case. This indicates a more negative value for cases with lower uranium enrichment.

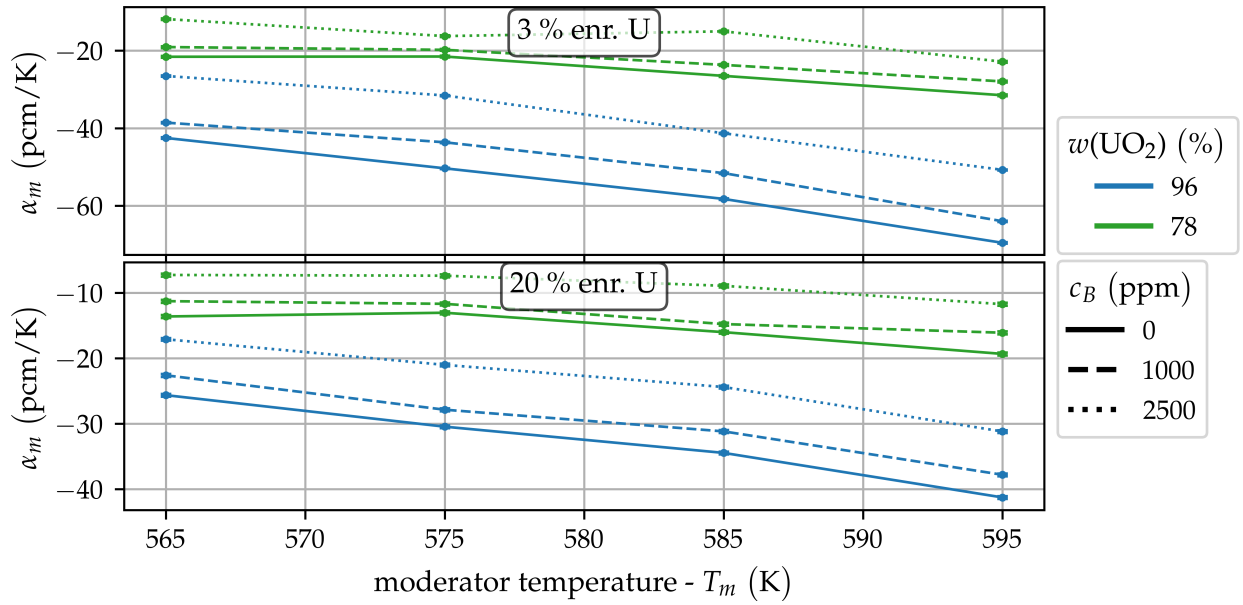

Figure 2. Moderator temperature feedback coefficient $\alpha_m(T_m)$, evaluated for two uranium enrichments, two UO_2 weight fractions, and three boron concentrations c_B in the water. Calculated values are shown as points with error bars, with lines included only to guide the eye.

As expected, a higher boron concentration results in a weaker α_m coefficient, which can become positive. This sets a limit in UO_2 fuel, as presented in [3], although this is not noticeable in the cases presented in this paper. The effect of boron is stronger (i.e., there is a larger difference between α_m for cases with and without boron) for a higher UO_2 weight fraction, while enrichment does not lead to significant differences between cases with or without boron.

Figure 4 shows the energy distribution of flux in the whole core across 600 energy groups. The shown cases were selected to span the widest possible range of the investigated parameter phase space. In the thermal region (approximately $E < 1\,\text{eV}$), the higher UO_2 weight fraction and lower uranium enrichment result in higher thermal flux, which leads to increased capture in ^{240}Pu and ^{242}Pu, making α_m more negative. In the epithermal region (approximately between 1 eV and a few tens of keV), important resonances of uranium and plutonium are present, which are crucial for changes in capture compared to fission. Spectrum hardening, i.e., a shift of flux to the resonance region, affects the ratio between fission and capture. The changes due to temperature variation are small. With added boron, the flux decreases in the thermal region. At higher temperatures, a slight spectrum hardening is observed, which is consistent with trends in α_m.

4. FUEL TEMPERATURE

As in the moderator study, the fuel temperature was varied from 560 K to 1080 K in approximately 100 K increments, while the moderator temperature was kept at 560 K. With the change in temperature, only the material temperature was altered, neglecting changes in density and leakage due to thermal expansion.

The results for the fuel temperature reactivity feedback coefficient, $\alpha_f(T_f)$, are shown in Figure 5. The coefficient is negative, with a slight trend of increasing magnitude as temperature increases. With higher uranium enrichment and a lower UO_2 weight fraction, the effect is weaker. This can again be explained by the fission and radiative capture reaction rates, which are shown in Figure 6.

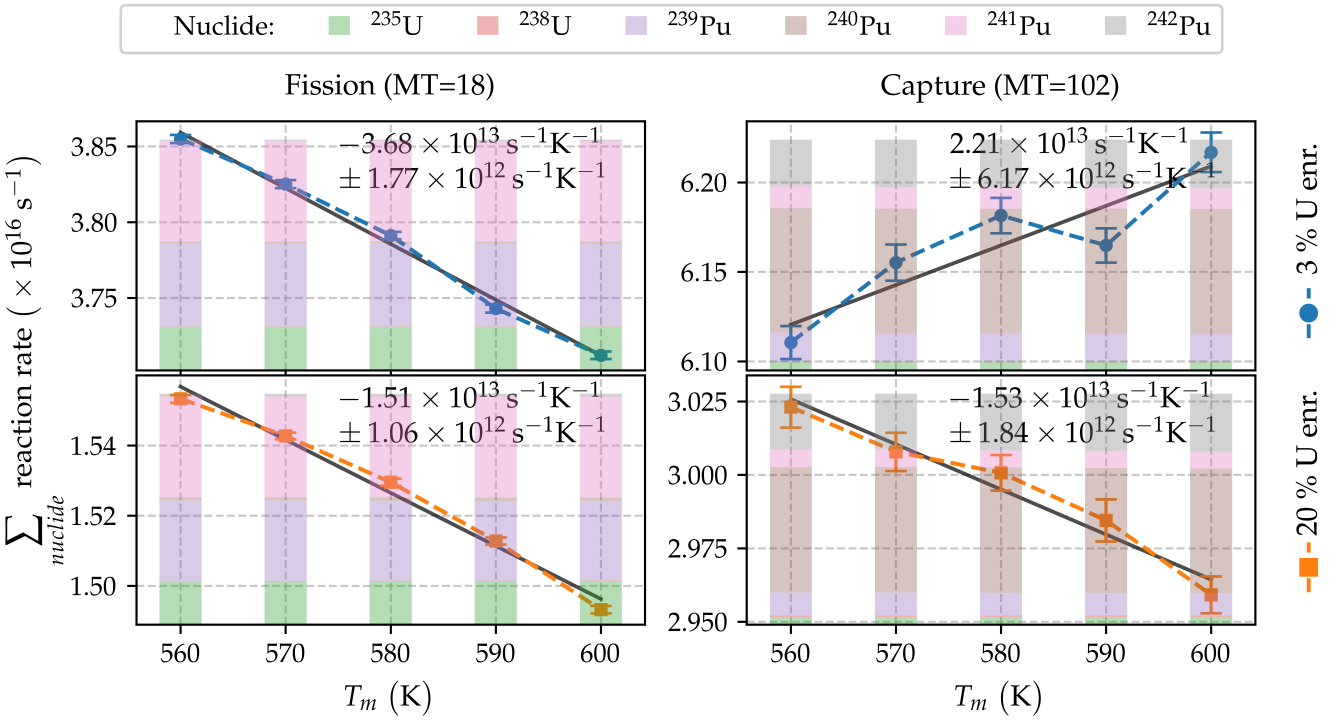

Figure 3. The sum of fission (left column) and capture (right column) reaction rates for the nuclides ^{235}U, ^{238}U, ^{239}Pu, ^{240}Pu, ^{241}Pu, and ^{242}Pu is shown for 3 % (upper row) and 20 % (lower row) uranium enrichment as coloured points connected with lines included only to guide the eye. A linear function was fitted to the individual data and is represented by a black line, with the slope value and its uncertainty indicated in the top right corner of each plot. Vertical bars show the relative contributions of individual nuclides for a specific moderator temperature. The bottom of each bar represents 0 %, and the top 100 %.

Figure 6 shows the sums of reaction rates for the nuclides ^{235}U, ^{238}U, ^{239}Pu, ^{240}Pu, ^{241}Pu, and ^{242}Pu for two cases of different uranium enrichment (3 % and 20 %). The highest fission reaction rates occur for ^{235}U, ^{239}Pu, and ^{241}Pu. The highest radiative capture rates are observed for ^{240}Pu and ^{242}Pu. The behaviour of the reaction rates with fuel temperature can be understood in terms of Doppler broadening of resonance cross sections. For both uranium and plutonium isotopes, an increase in fuel temperature broadens the resonances and enhances absorption in the epithermal energy range. For ^{235}U, ^{239}Pu, and ^{241}Pu, this additional absorption partly feeds fission, whereas for ^{240}Pu and ^{242}Pu, it predominantly increases radiative capture. As shown by the linear trends in Figure 6, the capture-rate slope increases with temperature while the fission-rate slope decreases, resulting in a net reduction in reactivity with increasing fuel temperature and hence a negative α_f. At 20 % enrichment, the capture-rate slope is approximately 2.4 times smaller than at 3 %, and the reduced relative importance of plutonium resonances further accounts for the less negative fuel-temperature coefficient in this case.

The changes in the energy distribution of flux in the thermal region are not as pronounced as those observed when varying the moderator temperature. Instead, they occur in the resonance region (around 1 eV to several tens of keV), where increasing fuel temperature leads to Doppler broadening of the resonances and, consequently, higher absorption. At higher enrichment, the differences become smaller because absorption is distributed differently between uranium and plutonium. As shown in Figure 6, the fission reaction rate decreases with increasing T_f, but capture reactions increase significantly, especially at lower enrichment and higher weight fractions of UO_2. In the resonance region, the neutron flux locally decreases as the broadened resonance peak results in more absorption, which appears as

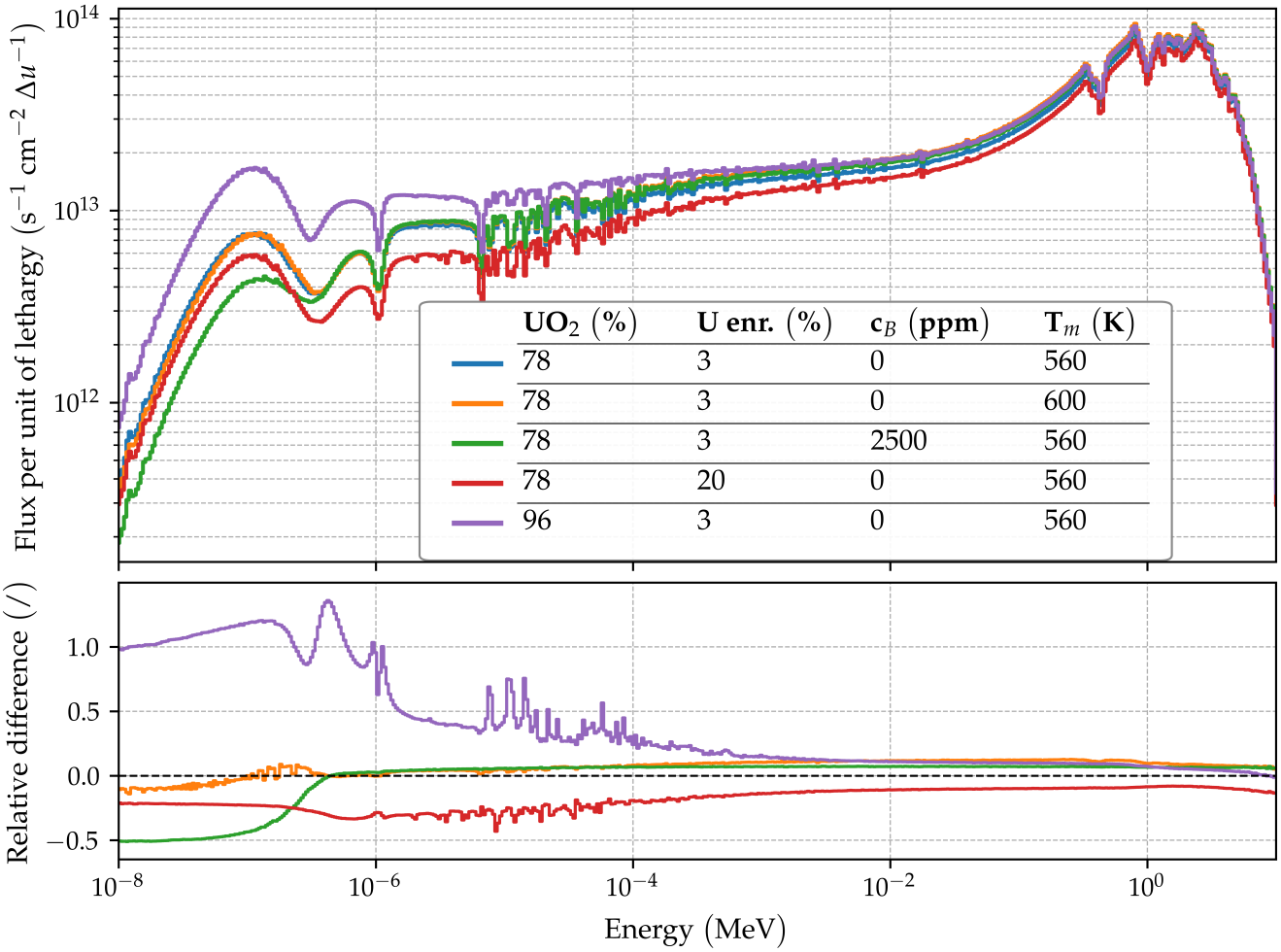

Figure 4. Flux distribution per unit of lethargy Δu, defined as $\Delta u = \ln\left(E_{high}/E_{low}\right)$, where E_{low} and E_{high} are the boundaries of each energy group. Below is shown the relative difference from the distribution for the case with the lowest UO_2 weight fraction, uranium enrichment, and T_m (blue line in the upper plot).

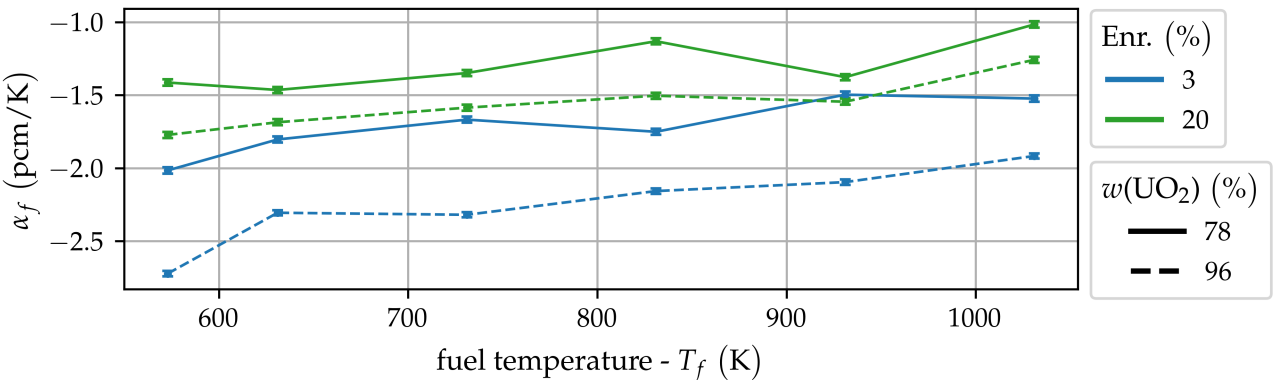

Figure 5. Fuel temperature feedback coefficient $\alpha_f(T_f)$, evaluated for two uranium enrichments and two UO_2 weight fractions. Calculated values are shown as points with error bars, with lines included only to guide the eye.

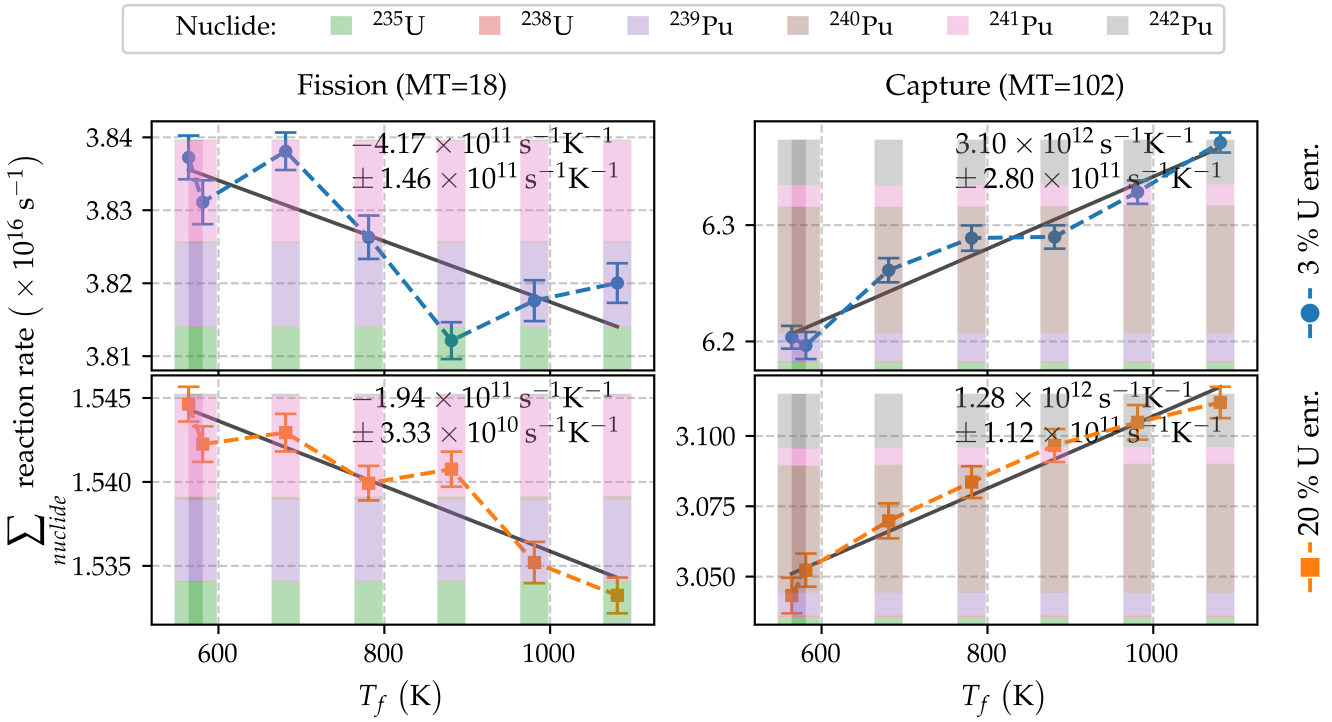

Figure 6. The sum of fission (left column) and capture (right column) reaction rates for the nuclides ^{235}U, ^{238}U, ^{239}Pu, ^{240}Pu, ^{241}Pu, and ^{242}Pu is shown for 3 % (upper row) and 20 % (lower row) uranium enrichment as coloured points connected with lines included only to guide the eye. A linear function was fitted to the individual data and is represented by a black line, with the slope value and its uncertainty indicated in the top right corner of each plot. Vertical bars show the contributions of individual nuclides for a specific fuel temperature. The bottom of each bar represents 0 %, and the top 100 %.

an increase in capture (Figure 6). The net effect is increased neutron capture by ^{240}Pu and ^{242}Pu, both of which are non-fissile, resulting in reduced reactivity and hence a more negative α_f. Uranium enrichment and the UO_2 weight fraction have the same effect on the spectrum as described in Section 3. Higher uranium enrichment leads to more fission occurring in ^{235}U, and the different absorption energy distribution means that spectrum changes with T_f are less pronounced. A UO_2 weight fraction results in a larger share of uranium resonances, resulting in a stronger Doppler effect and greater spectrum change with variation in T_f. In fuel with lower enriched uranium and a high weight fraction of UO_2, the coefficient α_f is more negative than at higher enrichment and lower proportion.

5. CONCLUSIONS

The results show that uranium enrichment, the UO_2 weight fraction in MOX, and the boron concentration in the coolant all significantly affect the temperature feedback coefficients.

In all cases studied (uranium enrichment up to 20 %, UO_2 weight fraction between 78 % and 96 %, and boron concentration up to 2500 ppm), the limit of $\alpha_m > 0$ was never reached or exceeded. The amount of uranium and its enrichment influence the magnitude of α_m. Higher uranium enrichment and a lower weight fraction of UO_2 weaken the coefficient, as both reduce the temperature dependence slope of the radiative capture reaction rate. The presence of boron also weakens the coefficient, but within the parameter range considered, it never becomes positive, even at the highest concentration.

The fuel temperature coefficient, α_f, was negative in all cases studied. The uranium enrichment and

UO_2 weight fraction in the fuel affect the magnitude of α_f. For fuel with higher uranium enrichment and a lower UO_2 weight fraction, the coefficient is weaker (less negative). This is due to a slower change in the radiative capture reaction rate with temperature in these cases.

This study provides a foundation for further investigation of MOX fuel, water coolant, and their suitability for the DARWIN reactor core concept. Future work will include studies of changes in flux distribution, power peaking factors, core geometry variations with changing pin pitch, and the inclusion of additional reactivity control mechanisms. This study represents a small part of the exploration of phase space limits, which should serve as a reference point for future research on optimisation problems using genetic algorithms or artificial intelligence.

ACKNOWLEDGEMENTS

The authors acknowledge financial support from the Slovenian Research and Innovation Agency (research core funding No. P2-0073 Reactor Physics and the project PR-12841 Training of young researchers) and RSF-funding scheme through the project "SMARTI (Small ModulAr Reactor Technology Innovation / Tehnološka inovacija majhnega modularnega reaktorja)"

REFERENCES

[1] "Dispatchable Adaptive Reactor With Interchangeable compoNents (DARWIN)." URL https://darwin.ijs.si/.

[2] G. Locatelli, A. Fiordaliso, S. Boarin, and M. E. Ricotti. "Cogeneration: An option to facilitate load following in Small Modular Reactors." *Progress in Nuclear Energy*, **volume 97**, pp. 153–161 (2017). URL https://www.sciencedirect.com/science/article/pii/S014919701630292X.

[3] A. Mihelčič, D. Čalič, and L. Snoj. "DARWIN Reactor Core: Fuel and Moderator Temperature Feedback." In *Proceedings of the 34th International Conference Nuclear Energy for New Europe*. Ljubljana, Slovenia (2025). To appear.

[4] Leppänen, Jaakko, Valtavirta, Ville, Rintala, Antti, and Tuominen, Riku. "Status of Serpent Monte Carlo code in 2024." *EPJ Nuclear Sci Technol*, **volume 11**, p. 3 (2025). URL https://doi.org/10.1051/epjn/2024031.

[5] M. Chadwick, M. Herman, P. Obložinský, et al. "ENDF/B-VII.1 Nuclear Data for Science and Technology: Cross Sections, Covariances, Fission Product Yields and Decay Data." *Nuclear Data Sheets*, **volume 112**, pp. 2887 – 2996 (2011). URL https://doi.org/10.1016/j.nds.2011.11.002.

[6] A. Mihelčič, D. Čalič, and L. Snoj. "Adaptive design and criticality analysis of the DARWIN reactor core concept." In *Proceedings of the 33rd International Conference Nuclear Energy for New Europe*. Nuclear Society of Slovenia, Ljubljana, Slovenia (2024).

[7] A. Mihelčič, D. Čalič, and L. Snoj. "A study of temperature feedback in the DARWIN core concept with comparison of Monte Carlo and deterministic approaches." In *International Conference on Mathematics and Computational Methods Applied to Nuclear Science and Engineering (M&C 2025)*, pp. 912–921. American Nuclear Society, Illinois (2025).

[8] E. W. Lemmon, I. H. Bell, M. L. Huber, and M. O. McLinden. "Thermophysical Properties of Fluid Systems." In P. Linstrom and W. Mallard, editors, *NIST Chemistry WebBook, NIST Standard Reference Database Number 69*. National Institute of Standards and Technology, Gaithersburg MD, 20899.

[9] R. S. Detwiler, R. J. McConn, T. F. Grimes, S. A. Upton, and E. J. Engel. "Compendium of Material Composition Data for Radiation Transport Modeling." Technical report, Pacific Northwest National Laboratory (PNNL), Richland, WA (United States) (2021). URL https://doi.org/10.2172/1782721.